

3-Dimensional Mapping of Corneal Topography and Thickness

Jose B. Almeida and Sandra Franco

Universidade do Minho, Departamento de Física, 4710-057 Braga, Portugal.

(Dated: April 17, 2024)

An optical system that provides topographical maps of both external and internal corneal surfaces as well as the latter's thickness map is here described. Optical sections of the cornea are obtained by illumination with a collimated beam expanded in a fan shape by a small rotary cylindrical lens. The light detected from the cornea is observed by two cameras and processed in order to yield the surfaces' profiles.

The optical system used to project a thin rotating line on the cornea consists of a white light source provided with optical fiber bundle output which is first conditioned by a set of lenses so that it would produce a spot on the cornea. A small cylinder lens is used to expand the beam in one direction so that a thin line illuminates the cornea, rather than a spot. The cylinder lens is provided with motor driven rotation about an axis normal to its own in order to rotate the line on the cornea such that the projected line scans the whole cornea; the illuminator is completed with a slit aperture.

The cornea is not perfectly transparent, scattering some of the light that traverses it; this fact is used for its observation by two cameras. These are placed at pre-defined angles with the illumination axis, so that optical sections of the cornea can be seen; the use of two cameras avoids the need for camera rotation in synchronism with the cylinder. The two cameras' images can be combined in order to simulate a single virtual rotating camera.

Image processing is used to extract information about the corneal surfaces profiles and thickness from the optical sections. Several peculiar aspects of processing are discussed, namely the corneal edge detection algorithm, the correction for angle of view and deformation due to observation of the inner surface through the cornea.

PACS numbers: 42.66.Ct; 42.30.-d; 87.57.-s.

I. INTRODUCTION

With the advent of refractive surgery precise corneal pachymetry thickness has become increasingly important, as parameters related to corneal shape and thickness must be accurately measured in order to ensure safety and accuracy ever more complex interventions. Knowledge of corneal thickness is also useful when studying corneal pathological conditions such as keratoconus, [1, 2, 3] investigating corneal physiology [4, 5] and in contact lens research. [6, 7, 8, 9, 10]

Many pachymetry techniques have been developed for the determination of central corneal thickness, with optical pachymetry the most commonly used. However, this technique is slow and the results are subjective because the operator must operate the doubling device, estimating the point at which the lines corresponding to the two corneal surfaces either just touch or overlap, depending on the method used. On the other hand ultrasonic pachymeters do not require much training and produce more rapid and objective results, although they require an anesthetized cornea, forbidden to some practitioners in some countries. New pachymetric methods based on optical technology have recently been developed and clinically applied, some of them providing pachymetric maps and not only central

thickness. Confocal microscopy, videopachymetry, three-dimensional topography marketed as Orbscan, optical tomography, non-contact and contact specular microscopy, and low-coherence interferometry are other techniques used in the measurement of corneal thickness. A review of these methods has been published. [11]

The authors developed an optical corneal tomographer that uses two CCD cameras and an innovative illuminating system that allows thickness measurements along any desired meridian and also motorized scanning of the entire cornea. The optical principles and technical details of a precursor apparatus have been described. [12, 13, 14]

II. SYSTEM DESCRIPTION

The optical part of the system consists of an illuminator and two CCD cameras (COU 2252) provided with 55 mm telecentric lenses; this is complemented by an appropriate headrest and data processing computer. Fig. 1 shows a picture of the optical components, where it is possible to see the special arrangement of illuminator and the two cameras.

The illuminator is aligned with the visual axis and comprises a quartz halogen light source an optical fiber bundle, a collimator, a small cylindrical lens, a convex lens and an apodizing aperture slit, see Fig. 2. After the beam is collimated, a small cylindrical lens expands it in a fan. This lens has the shape of a rod with a diameter of 5 mm and is held in a mount that can be rotated to

Electronic address: bda@fisica.uminho.pt

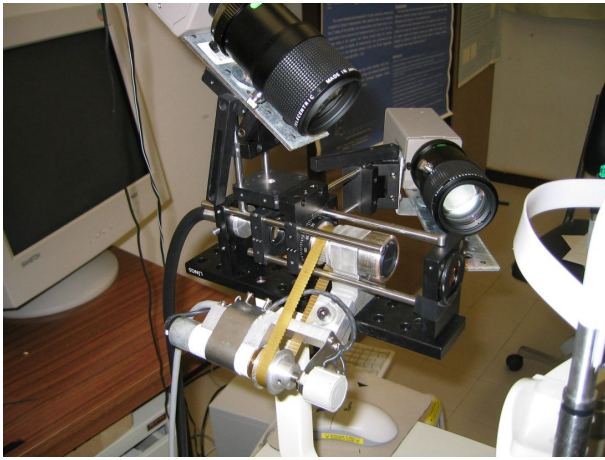


FIG .1: View of the optical components; notice the two cameras and the illuminator.

produce rotary scanning of all of the cornea. The fan is then focused on the corneal surface by a convex lens projecting a thin strip of light whose orientation follows the cylinder lens' orientation.

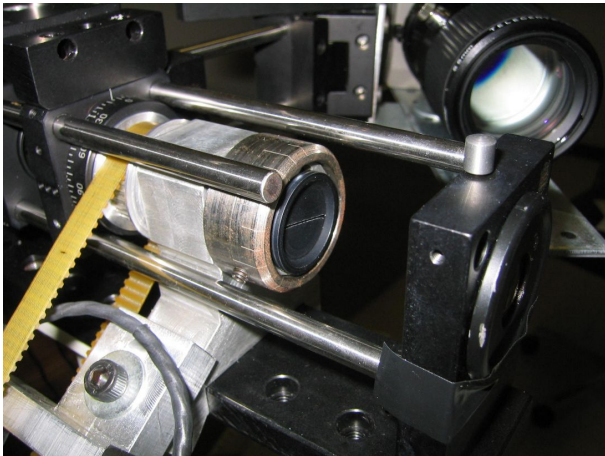


FIG .2: Detailed view of the illuminator showing the rotation mechanism and the apodizing slit.

The light di used by both surfaces and the inner cornea is collected by two video cameras placed at 60° with the light beam and defining with the visual axis planes perpendicular to each other. Each camera sees an image similar to Fig. 3, where the cornea appears as a gray area in with the shape of an arc; in the original colored image the cornea appears in dark blue and can be easily distinguished from the iris, which is usually shown in different color, frequently bright orange. Obviously the arc's orientation depends on the camera and on the cylinder lens' orientation, as shown in Fig. 4. The data of the two cameras is then used to compute the corneal thickness. The two cameras act like a single virtual camera that can be rotated with the cylinder lens; the advantage of using two cameras is that it allows



FIG .3: Vertical section of an eye showing the cornea as a grey arc; the iris can be seen as the white saturated area with the lens sitting in the center.

faster rotation scanning then would be possible if a single camera had to be rotated in synchronism with the lens.

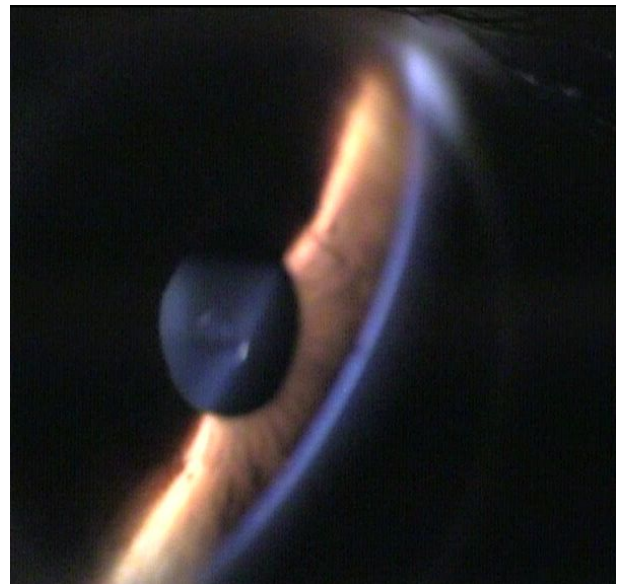


FIG .4: Oblique section of the cornea obtained by the camera on the horizontal plane when the projected light strip makes an angle of approximately 45° with the vertical direction.

Figure 5 illustrates the working principle. A light beam incident on the cornea is scattered on the inside and the scattered light can be observed at an angle to the incidence direction; since a corneal meridian is illuminated the scattered light produces the arc shape already men-

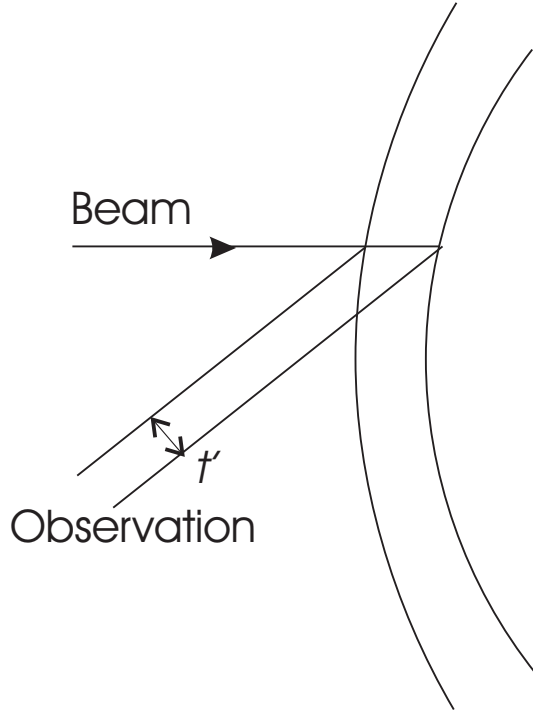


FIG. 5: Working principle: the illuminating beam traverses the cornea and scattered light is observed at an established angle; the observed thickness t^0 is apparent and must be corrected by software.

tioned. The shape and width of the arc have information about the cornea's shape and thickness but data processing is needed to retrieve the correct values for those parameters.

III. DATA PROCESSING

A considerable amount of processing is necessary in order to recover the true shape and thickness of the cornea from the cameras' images we will detail the various steps below. Fortunately processing speed is not important because all the collected data can be saved for later processing, reducing considerably the observation time.

The illustration in Fig. 3 was obtained by the camera laying on the horizontal plane when the projected light strip was vertical; this image depicts a vertical section of the cornea and the corresponding image on the vertical camera carries no information because it is reduced to a bright straight line. The situation is reversed when the projected strip is horizontal but for all other situations there is information in both images, which must be processed in order to obtain the image that would be seen by a virtual camera on a plane always normal to the projected strip. The first processing step consists in the application of simple trigonometric rules to recover the virtual camera's image.

The second processing step consists in detecting the

edges of the gray arc in image of the cornea using the method known as "adaptive thresholding" reported by Hachicha et al. [15]. The procedure involves the analysis of the gray-level along a scan line crossing the corneal image and comparing this to a predefined threshold level. A pixel P_i is selected as an "edge point," when it verifies the two simultaneous conditions:

$$\begin{aligned} I(P_i) &= I_{min} + 0.5(I_{max} - I_{min}) \\ I(P_{i-1}) &< I_{min} + 0.5(I_{max} - I_{min}) \end{aligned} \quad (1)$$

where the pixels are ranked from 1 to N across the profile, $I(P_i)$ is the gray-level at pixel P_i and I_{min} , I_{max} are the gray-level minimum and maximum, respectively. Hachicha et al. [15] used a threshold of 0.3 ($I_{max} - I_{min}$) in their work but we found that increasing the factor from 0.3 to 0.5 gave us more reliable results. The discrete edge points are then joined by spline fitting, allowing determination of the normal direction and apparent thickness measured along that direction.

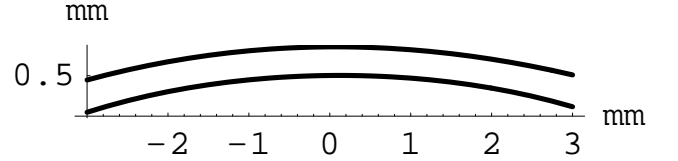


FIG. 6: Corneal profile along a vertical meridian obtained by edge detection and spline fitting on the acquired image.

The corneal thickness was computed from the distance between the two edge profiles affected by corrections to allow for the observation angle and corneal curvature. The former of these corrections was detailed in previous work [14] and consists only in dividing the apparent thickness by the sine of the observation angle; the latter was performed considering the optical magnification produced by an average curvature and could be improved by iterative processing, using pre-determined curvature at each point. We are presently developing the software for data display in the form of topographical and pachymetric maps; for the moment we can produce profile and thickness graphics along any chosen meridian, as illustrated in Figs. 6 and 7.

IV. CONCLUSION

The authors describe a novel optical system designed to provide topographical maps of both corneal surfaces and corneal pachymetry. Although not fully developed the system is already capable of delivering clinically meaningful information, relevant for diagnosis and surgery.

The authors describe the optical system used to project a thin rotating line on the cornea. This is obtained with a white light source provided with optical fiber bundle output; the light from the fiber bundle is first conditioned

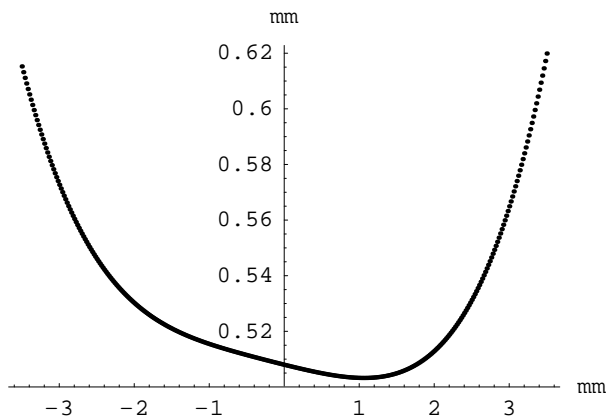


FIG. 7: Corneal thickness from the profile in Fig. 6 vs. distance from the visual axis.

by a set of lenses so that it would produce a spot on the cornea. A small cylinder lens is used to expand the beam in one direction so that a thin line illuminates the cornea,

rather than a spot. The cylinder lens is provided with motor driven rotation about an axis normal to its own in order to rotate the line on the cornea such that the projected line scans the whole cornea.

The cornea is not perfectly transparent, scattering some of the light that traverses it; this fact is used for its observation by two cameras. These are placed at predefined angles with the illumination axis, so that optical sections of the cornea can be seen; the use of two cameras avoids the need for camera rotation in synchronism with the cylinder. The two cameras' images can be combined in order to simulate a single virtual rotating camera.

Image processing was used to extract information about the corneal surfaces profiles and thickness from the optical sections. Several peculiar aspects of processing were presented and discussed, namely the corneal edge detection algorithm, the correction for angle of view and deformation due to observation of the inner surface through the cornea. Some examples of observed corneal profiles were shown.

-
- [1] M. A. Parata, J. M. Gonzalez-Mejia, J. A. Diaz, and E. Yebra-Pimentel, *Arch. Soc. Esp. Ophthalmol.* 75, 633 (2000).
 - [2] R. B. Mandell and K. A. Polse, *Arch. Ophthalmol.* 82, 182 (1969).
 - [3] C. Edmund, *Acta Ophthalmol.* 65, 145 (1987).
 - [4] A. Tomlinson, *Acta Ophthalmol.* 50, 73 (1972).
 - [5] S. G. El Hage and C. Beaulieu, *Am. J. Optom. Physiol. Opt.* 50, 863 (1973).
 - [6] R. K. Rivera and K. A. Polse, *Optom. Vis. Sci.* 73, 178 (1996).
 - [7] T. L. Sanders, K. A. Polse, M. D. Sarver, and M. G. Harris, *Am. J. Optom. Physiol. Optics* 52, 393 (1975).
 - [8] J. A. Bonanno and K. A. Polse, *Am. J. Optom. Physiol. Opt.* 62, 74 (1985).
 - [9] B. A. Holden, D. F. Sweeney, A. Vannas, K. T. Nilsson, and N. Efron, *Invest. Ophthalmol. Vis. Sci.* 26, 1489 (1985).
 - [10] B. A. Holden, J. J. McNally, G. W. Mertz, and H. A. Swarbrick, *Acta Ophthalmol.* 63, 684 (1985).
 - [11] M. A. Parata, E. Yebra-Pimentel, M. J. Gonzalez, J. Gonzalez-Perez, J. M. Gonzalez-Mejia, and A. Cervino, in *Recent Research Developments in Optics*, edited by S. G. Pandey (Research Signpost, India, 2002), pp. 33{51.
 - [12] S. Franco, J. B. Almeida, and M. Parata, *J. Refract. Surg.* 16, S661 (2000), re-printed from [16].
 - [13] S. Franco, J. B. Almeida, and M. Parata, in *Vision Science and its Applications (VSIA)* (Optical Society of America, Monterey, California, USA, 2001), pp. 148{151.
 - [14] S. Franco, J. B. Almeida, and M. Parata, in *3rd International Congress of Wavefront Sensing and Aberration-Free Refractive Correction* (Interlaken, Switzerland, 2002), vol. 18 of *J. Refract. Surg.*, pp. S630{S633.
 - [15] A. Hachicha, S. Simon, J. Samson, and K. Hanna, *Comput. Vision Graphics Image Process.* 47, 131 (1989).
 - [16] S. Franco, J. B. Almeida, and M. Parata, in *Vision Science and its Applications*, edited by V. Lakshminarayanan (OSA, Washington D.C., 2000), vol. 35 of *Topics in Optics and Photonics Series*, pp. 297{301.